Cell Reports

Report

A UV-Independent Topical Small-Molecule Approach for Melanin Production in Human Skin

Graphical Abstract

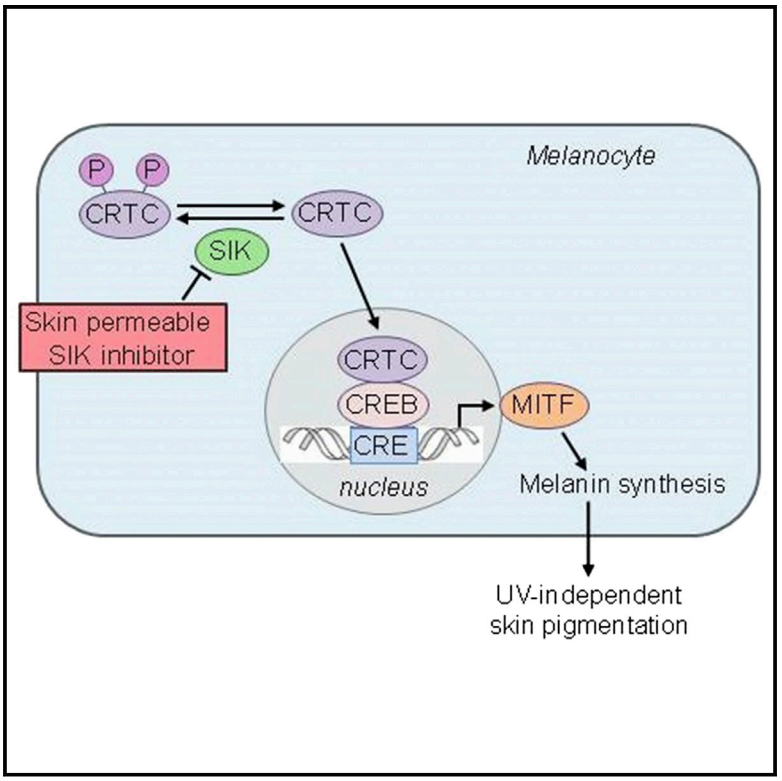

Authors

Nisma Mujahid, Yanke Liang, Ryo Murakami, ..., Elisabeth M. Roider, Nathanael S. Gray, David E. Fisher

Correspondence

dfisher3@mgh.harvard.edu

In Brief

Mujahid et al. describe the successful generation of topical small molecules capable of inducing dark pigmentation in human skin, thus potentially generating a variety of new applications.

Highlights

- SIK inhibitors induce *MITF*, the master regulator of pigment genes in vitro
- Topical SIK inhibitor treatment of redhead mice rescues melanin production
- Human skin-permeable SIK inhibitors induce melanin production in human skin explants

Mujahid et al., 2017, Cell Reports *19*, 2177–2184
June 13, 2017
http://dx.doi.org/10.1016/j.celrep.2017.05.042

CellPress

Cell Reports
Report

A UV-Independent Topical Small-Molecule Approach for Melanin Production in Human Skin

Nisma Mujahid,[1,2,5] Yanke Liang,[3,4,5] Ryo Murakami,[2] Hwan Geun Choi,[3,4] Allison S. Dobry,[2] Jinhua Wang,[3,4] Yusuke Suita,[2] Qing Yu Weng,[2] Jennifer Allouche,[2] Lajos V. Kemeny,[2] Andrea L. Hermann,[2] Elisabeth M. Roider,[2] Nathanael S. Gray,[3,4] and David E. Fisher[2,6,*]

[1]Department of Pathology and Laboratory Medicine, Boston University School of Medicine, Boston, MA 02118, USA
[2]Cutaneous Biology Research Center, Department of Dermatology, Massachusetts General Hospital, Harvard Medical School, Charlestown, MA 02129, USA
[3]Department of Cancer Biology, Dana-Farber Cancer Institute, Boston, MA 02215, USA
[4]Department of Biological Chemistry and Molecular Pharmacology, Harvard Medical School, Boston, MA 02115, USA
[5]These authors contributed equally
[6]Lead Contact
*Correspondence: dfisher3@mgh.harvard.edu
http://dx.doi.org/10.1016/j.celrep.2017.05.042

SUMMARY

The presence of dark melanin (eumelanin) within human epidermis represents one of the strongest predictors of low skin cancer risk. Topical rescue of eumelanin synthesis, previously achieved in "redhaired" *Mc1r*-deficient mice, demonstrated significant protection against UV damage. However, application of a topical strategy for human skin pigmentation has not been achieved, largely due to the greater barrier function of human epidermis. Salt-inducible kinase (SIK) has been demonstrated to regulate MITF, the master regulator of pigment gene expression, through its effects on CRTC and CREB activity. Here, we describe the development of small-molecule SIK inhibitors that were optimized for human skin penetration, resulting in MITF upregulation and induction of melanogenesis. When topically applied, pigment production was induced in *Mc1r*-deficient mice and normal human skin. These findings demonstrate a realistic pathway toward UV-independent topical modulation of human skin pigmentation, potentially impacting UV protection and skin cancer risk.

INTRODUCTION

The incidence of nonmelanoma and melanoma skin cancers has been increasing in the United States over recent decades (Rogers et al., 2015; Ryerson et al., 2016; Watson et al., 2016). Epidemiological evidence suggests that there is a causal relationship between sun/UV exposure and the three major histologic forms of skin cancer: squamous cell carcinoma, basal cell carcinoma, and cutaneous melanoma (Gandini et al., 2005; Kennedy et al., 2003; Wu et al., 2014). Individuals with fair skin and/or poor tanning ability are at higher risk for developing these malignancies (Armstrong and Kricker, 2001), which are uncommon in darkly pigmented individuals (Pennello et al., 2000). During UV-induced tanning, DNA damage in keratinocytes triggers p53-mediated transcription of the pro-opiomelanocortin (*POMC*) gene (Cui et al., 2007). Proteolytic cleavage of POMC produces alpha-MSH (melanocyte-stimulating hormone), which binds to the melanocortin-receptor-1 (MC1R) on melanocytes, activating adenylate cyclase. Elevated cyclic AMP (cAMP) activates protein kinase A (PKA), which phosphorylates the cAMP-responsive-element-binding protein (CREB) (Newton et al., 2005; Tsatmalia et al., 1999), which, in turn, stimulates the transcription of the microphthalmia-associated transcription factor (*MITF*) gene (Bertolotto et al., 1998; Price et al., 1998). *MC1R* non-signaling variants are associated with lighter skin tones and red hair and are linked to poor tanning responses (Valverde et al., 1995). Previously, topical application of the cAMP agonist forskolin was shown to rescue the cAMP-MITF-eumelanin pathway in *Mc1r*-deficient mice (D'Orazio et al., 2006). Subsequent studies identified the phosphodiesterase PDE4D3 as a key regulator of melanocytic cAMP homeostasis, and its suppression produced hyperpigmentation similar to forskolin treatment in red-haired mice (Khaled et al., 2010). However, attempts to apply both of these small-molecule approaches to human skin have been unsuccessful, likely related to poor skin penetration of the active species.

Genetic data in mice have suggested the presence of a pathway in which CREB-regulated transcription co-activator (CRTC) positively regulates and salt-inducible kinase 2 (SIK2) negatively regulates MITF and pigment synthesis independently of CREB phosphorylation by PKA (Horike et al., 2010). In macrophages, the small-molecule SIK inhibitor HG 9-91-01 has been shown to regulate CREB-dependent gene transcription by suppressing phosphorylation of CRTC (Clark et al., 2012), thereby inhibiting cytoplasmic sequestration and permitting its nuclear translocation. We hypothesized that small-molecule SIK inhibitors could be generated and optimized as topical agents capable of inducing cutaneous pigmentation independently of UV irradiation in human skin.

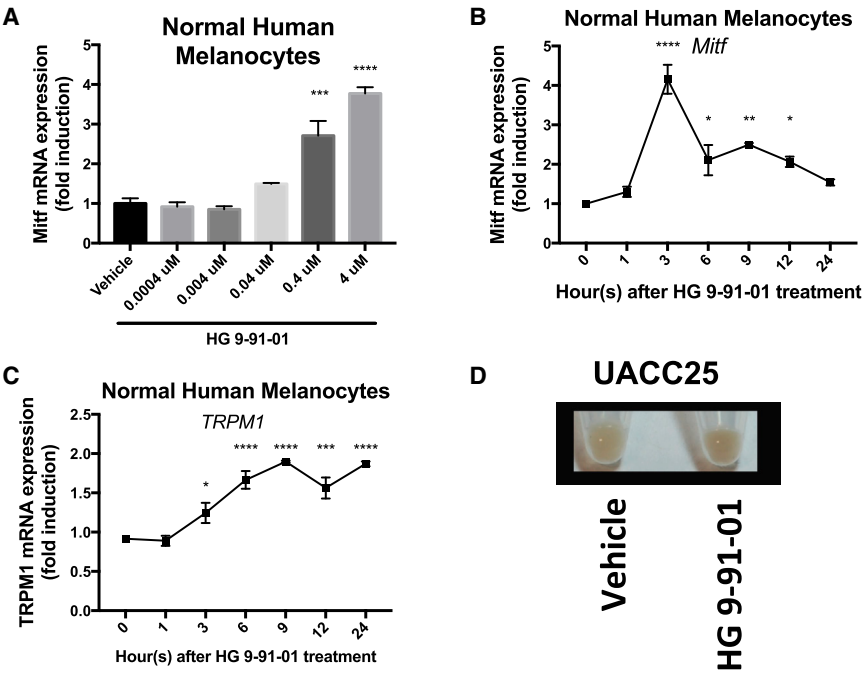

Figure 1. Inhibition of SIK by HG 9-91-01 Promotes *MITF* Transcription and Pigmentation In Vitro

(A) mRNA expression of *MITF* relative to *RPL11* mRNA and vehicle control in normal human melanocytes 3 hr after HG 9-91-01 or vehicle control (70% ethanol, 30% propylene glycol) treatment, quantified by qRT-PCR (n = 3, mean ± SEM).

(B and C) mRNA expression of *MITF* (B) and *MITF*-dependent gene *TRPM1* (C) relative to *RPL11* mRNA and vehicle control at each time point, in normal human melanocytes over 24 hr after 4 μM HG 9-91-01 or vehicle control treatment, quantified by qRT-PCR (n = 3, mean ± SEM).

(D) Cell pellets of UACC257 melanoma cells after 3 days of treatment with vehicle control or 4 μM SIK inhibitor HG 9-91-01 (image is representative of n = 3 experiments).

For the graph in (A), statistical significance is reported as follows: ***p < 0.001; ****p < 0.0001, one-way ANOVA with Dunnett's multiple comparisons test comparing treatment dose to vehicle control. For the graphs in (B) and (C), statistical significance is reported as follows: *p < 0.05; **p < 0.01; ***p < 0.001; ****p < 0.0001, repeated-measures one-way ANOVA with Dunnett's multiple comparisons test comparing each time point to time point 0.

RESULTS

Small-Molecule Inhibition of SIK Induces *MITF* Expression In Vitro

To test regulation of the pigmentation pathway by the previously published SIK inhibitor HG 9-91-01 (HG) (Clark et al., 2012) in vitro, we treated normal human melanocytes, UACC62 human melanoma cells, and UACC257 human melanoma cells. Dose-dependent increases in expression of *MITF* were observed in these cells in response to SIK inhibitor application (Figures 1A, S1A, and S1D). RNA levels of the MITF target gene *TRPM1* (Miller et al., 2004) also increased and followed the anticipated delayed kinetics relative to *MITF* induction in normal human melanocytes (Figures 1B and 1C) and UACC257 human melanoma cells (Figures S1G and S1H). Gross pigmentation was observed in cell pellets of UACC257 human melanoma cells after 3 days of HG 9-91-01 treatment (Figure 1D). Since SIK kinase activity is known to be dependent on LKB1 (Katoh et al., 2006) we next evaluated whether SIK-inhibitor treatment of LKB1-null G361 melanoma cells would induce MITF. In LKB1-null G361 melanoma cells, there is no *MITF* induction with SIK-inhibitor treatment (Figure S1J). In contrast, when LKB1 is introduced in G361 melanoma cells (Figure S1I), we observed a 6-fold induction of *MITF* expression with SIK-inhibitor treatment (Figure S1K), demonstrating the dependence of SIK-inhibitor effect on active SIK. These data suggest that small-molecule SIK inhibition can stimulate the pigmentation pathway in vitro.

HG 9-91-01 Rescues Melanogenesis in Mice with Inactive Melanocortin 1 Receptor

Since our in vitro results demonstrated that inhibition of SIK by HG 9-91-01 positively regulated *MITF* transcription, we next evaluated whether topical application of this compound could induce pigmentation independent of MC1R in vivo. To test this, we utilized a previously described mouse "red hair" model that carries the inactivating $Mc1r^{e/e}$ mutant allele and a transgene, K14-SCF, in which stem cell factor expression is driven by the keratin-14 promoter, allowing for epidermal homing of melanocytes (D'Orazio et al., 2006; Kunisada et al., 1998). Albino mice harboring a mutation in the *tyrosinase* gene were combined with the K14-SCF transgene ($Tyr^{c/c}$;K14-SCF mice) and served as controls to evaluate whether the pigmentation afforded by topical SIK inhibitor was dependent upon the canonical tyrosinase-melanin pathway. Daily application of the SIK inhibitor HG 9-91-01 for 7 days caused robust darkening in $Mc1r^{e/e}$;K14-SCF mice (Figures 2A and S2A). No visible change in skin pigmentation was observed in $Mc1r^{e/e}$;K14-SCF mice treated with vehicle or in $Tyr^{c/c}$;K14-SCF mice treated with vehicle or HG 9-91-01 (Figures 2A, S2A, and S2B). Reflective colorimetry analysis (Commission Internationale de l'Eclairage [CIE] L* white-black color axis (Park et al., 1999)) revealed significant darkening in $Mc1r^{e/e}$;K14-SCF mice treated with SIK inhibitor, but not in vehicle-treated $Mc1r^{e/e}$;K14-SCF mice or in $Tyr^{c/c}$;K14-SCF mice treated with either SIK inhibitor or vehicle control (70% ethanol, 30% propylene glycol) (Figure 2B). Fontana-Masson staining, a specialized melanin stain, revealed strong induction of melanin production in $Mc1r^{e/e}$;K14-SCF mice only in areas treated with HG 9-91-01 (Figures 2C and S2D) but no pigment induction in $Mc1r^{e/e}$;K14-SCF mice treated with vehicle (Figure 2C) or in albino ($Tyr^{c/c}$;K14-SCF) mice treated with either vehicle or SIK inhibitor (Figure S2C). Nuclear capping of melanin-laden melanosomes was observed within epidermal keratinocytes in $Mc1r^{e/e}$;K14-SCF mice treated with HG 9-91-01 (indicated by white arrows) and represents a known subcellular localization typical of physiologic skin pigmentation

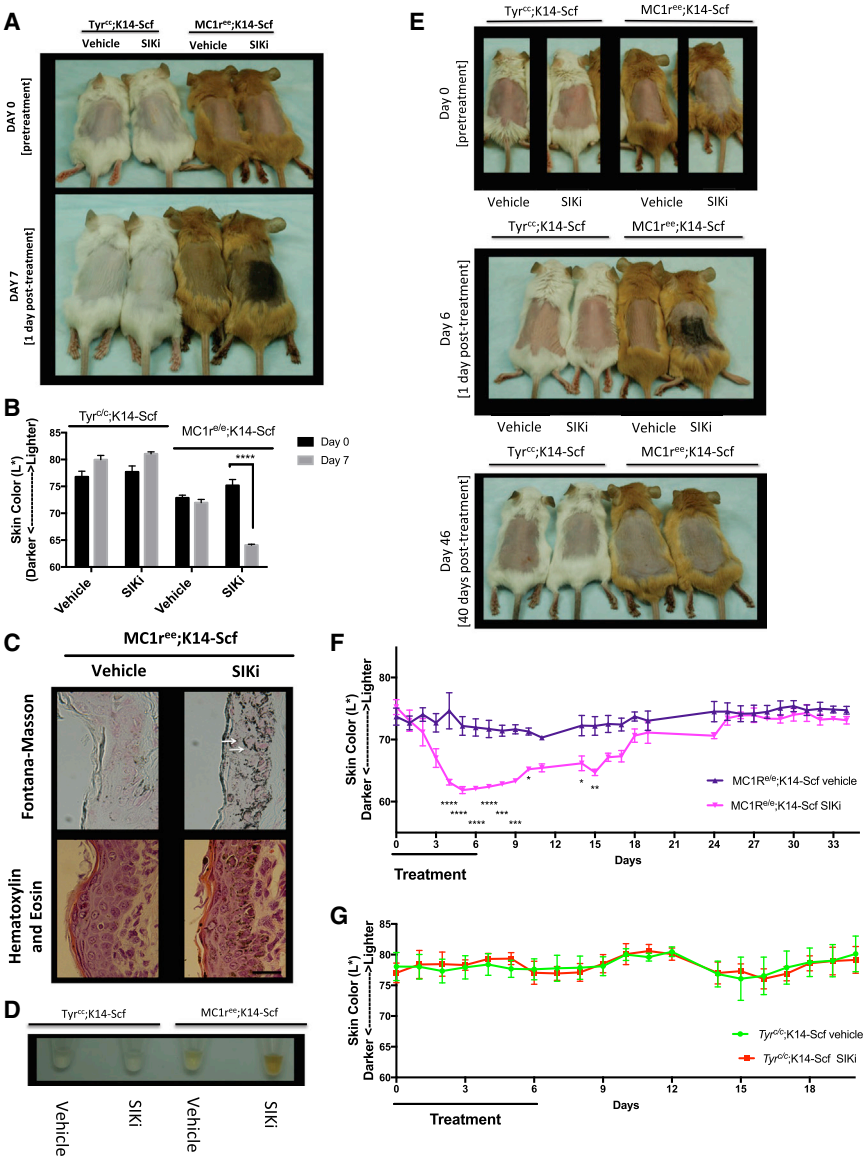

Figure 2. Topical Treatment with HG9-91-01 Causes Robust Darkening that Is Progressive and Reversible in *Mc1r*$^{e/e}$;K14-SCF Mice

(A–D) Shown here: (A) *Mc1r*$^{e/e}$;K14-SCF mice and *Tyr*$^{c/c}$;K14-SCF mice before treatment (day 0) and after 7 days of treatment (day 7) with 30 μL vehicle control (70% ethanol, 30% propylene glycol) or 37.5 mM HG 9-91-01 (image is representative of n = 4 experiments). (B) Reflective colorimetry measurements (L* white-black color axis; n = 4, mean ± SEM) and (D) melanin extraction (image is representative of n = 4 experiments) of the *Mc1r*$^{e/e}$;K14-SCF mice and *Tyr*$^{c/c}$;K14-SCF mice described in (A). (C) Skin sections of *Mc1r*$^{e/e}$;K14-SCF mice described in (A) stained with Fontana-Masson (eumelanin) (top two panels) or H&E (bottom two panels); (magnification, 400×). White arrows represent nuclear capping; scale bar represents 25 μm.

(E) *Mc1r*$^{e/e}$;K14-SCF mice and *Tyr*$^{c/c}$;K14-SCF mice before treatment (day 0) and after 6 days of treatment with 30 μL vehicle control (70% ethanol, 30% propylene glycol) or 37.5 mM HG 9-91-01 (day 6), and 40 days post-treatment (day 46) (vehicle mouse in day-46 photo is different from that in the day-0 and day-6 photos).

(F and G) Reflective colorimetry measurements (CIE L* white-black color axis) of (F) *Mc1r*$^{e/e}$;K14-SCF mice and (G) *Tyr*$^{c/c}$;K14-SCF mice treated as described in (E). Vehicle-treated *Mc1r*$^{e/e}$;K14-SCF mice: n = 5 (days 0–19), and n = 4 (days 24–34); HG 9-91-01-treated *Mc1r*$^{e/e}$;K14-SCF mice: n = 3; vehicle-treated *Tyr*$^{c/c}$;K14-SCF mice: n = 3 (days 0–10), and n = 2 (days 11–20); HG 9-91-01-treated *Tyr*$^{c/c}$;K14-SCF mice: n = 3 (mean ± SEM).

For the graph in (B), statistical significance is reported as follows: ****$p < 0.0001$, multiple t test analysis with the two-stage linear step-up procedure of Benjamini, Krieger, and Yekutieli. For the graphs in (F) and (G), statistical significance is reported as follows: *$p < 0.05$; **$p < 0.01$; ***$p < 0.001$; ****$p < 0.0001$, two-way ANOVA with Sidak's multiple comparisons test comparing treatment to vehicle control at each time point.

(Kobayashi et al., 1998) (Figure 2C). This feature suggests that SIK-inhibitor treatment stimulates not only melanocytic pigment synthesis but also the export of melanin in a fashion that closely mimics the known pathway of UV melanogenesis. H&E staining revealed normal morphology of HG 9-91-01-treated *Mc1r*$^{e/e}$;K14-SCF (Figure 2C) and *Tyr*$^{c/c}$;K14-SCF epidermis (Figure S2C). NaOH lysis of skin samples (Wakamatsu and Ito, 2002) revealed a visible increase in extractable eumelanin from *Mc1r*$^{e/e}$;K14-SCF mice treated with HG 9-91-01, compared with all other treatment groups (Figure 2D).

Darkening induced by topical application of HG 9-91-01 to *Mc1r*$^{e/e}$;K14-SCF mice was progressive over 6 days of treatment and gradually reversed over the 2 weeks after treatment was stopped (Figure 2F). Skin pigmentation remained in its pretreatment state 26 days later (40 days after treatment ended) (Figure 2E). No change was observed in *Tyr*$^{c/c}$;K14-SCF mice during treatment or 14 days after treatment was stopped (Figure 2G). Forty days after treatment was stopped, Fontana-Masson staining of skin sections of *Mc1r*$^{e/e}$;K14-SCF mice and Tyr$^{c/c}$;K14-SCF mice revealed no differences between vehicle and treatment groups, and H&E staining illustrated normal morphology for all mice (Figure S2E). These findings combined with the small-molecule and lipophilic nature of the SIK inhibitors led us to further investigate the use of SIK inhibitors for topical eumelanization of human skin.

Second-Generation SIK Inhibitors Are as Efficacious in Inducing the Pigmentation Pathway as HG 9-91-01

Since there are limitations to topical delivery of HG 9-91-01 into human skin epidermis (Figures 4A–4D), we derived SIK inhibitors designed to enhance passive epidermal permeation utilizing Lipinski's Rule of Five, which predicts greater absorption of

A

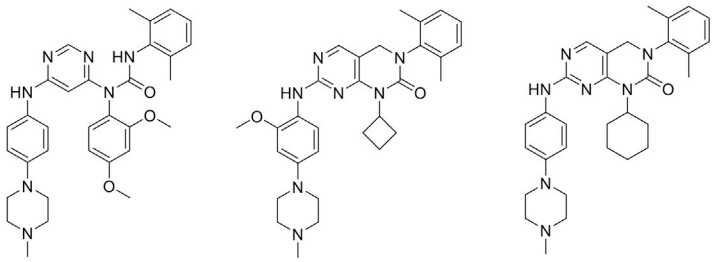

HG-9-91-01
SIK1/2/3: 4.29/4.02/8.37 nM

YKL-06-061
SIK1/2/3: 6.56/1.77/20.5 nM

YKL-06-062
SIK1/2/3: 2.12/1.40/2.86

B

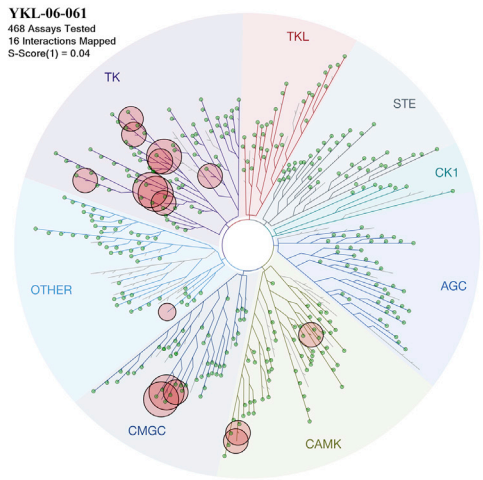

C

Kinase	% control at 1 μM	Enzymatic IC_{50} (nM)
CSF1R	0	9.66
FRK	0	1.10
KIT	0	153
p38-alpha	0	10.1
p38-beta	0	9.64
SRC	0.15	58.8
BRK	0.2	24.1
PDGFRB	0.25	103
EPHB1	0.3	16.4
SIK1	0.3	6.56
TNK2	0.4	10.5
RSK4	0.6	>10000
SIK2	0.7	1.77
NLK	0.95	132
PRKR	1	>10000

Figure 3. Characterization of SIK Inhibitors

(A) Structures of HG-9-91-01, YKL-06-061, and YKL-06-062 and their biochemical IC_{50}s against SIKs.

(B) KinomeScan kinase selectivity profile for YKL-06-061. YKL-06-061 was profiled at a concentration of 1 μM against a diverse panel of 468 kinases by DiscoverX. Kinases that exhibited a score of 1 or below are marked in red circles. (Score is percent relative to DMSO control. Smaller numbers indicate stronger binding.) See Table S1 for full kinome profile.

(C) Biochemical kinase IC_{50}s of YKL-06-061 top hits as shown in (B).

TK, tyrosine kinase; TKL, tyrosine kinase-like; STE, homologs of yeast sterile 7, sterile 11, sterile 20 kinases; CK1, casein kinase 1; AGC, containing PKA, PKG, and PKC families; CAMK, calcium/calmodulin-dependent protein kinase; CMGC, containing CDK, MAPK, GSK3, and CLK families. See also Table S1.

compounds if they have fewer than five H-bond donors, fewer than ten H-bond acceptors, a molecular weight less than 500 g/mol, and calculated log P (CLogP) less than 5 (Bos and Meinardi, 2000; Choy and Prausnitz, 2011; Lipinski et al., 2001) (Figure S3A). In an initial screen, two second-generation SIK inhibitors, YKL 06-061 and YKL 06-062, induced darkening as measured by reflective colorimetry analysis after topical treatment of human breast skin explants (Figure S3B). Furthermore, both YKL 06-061 and YKL 06-062 have a lower molecular weight than HG 9-91-01, and the more efficacious YKL 06-061 has a lipophilicity closer to Lipinski's Rule of Five, possibly explaining the drug's enhanced penetration capabilities (Figure S3A). Second-generation inhibitors had half maximal inhibitory concentration (IC_{50}) values for the inhibition of SIK1, SIK2, and SIK3 that were comparable to those of HG 9-91-01 (Figure 3A). To assess the kinome selectivity information of new analogs, YKL-06-061 was screened across a panel of 468 human kinases at a concentration of 1 μM using the KinomeScan methodology (DiscoverX). YKL-06-061 exhibited an S(1) score of 0.02, with 16 kinases displaying tight binding to it (Ambit scores of ≤ 1) (Figure 3B). As the KinomeScan assays measure binding, we also performed enzymatic assays for these targets either in house or using the SelectScreen Kinase Profiling Service at Thermo Fisher Scientific (Figure 3C). YKL-06-061 inhibited only one kinase, fyn-related kinase (FRK), more strongly than SIKs, which demonstrates its high overall selectivity (Figure 3C). We anticipate that YKL-06-062 has similar kinase selectivity, considering their high structural similarity. Similar to observations with HG 9-91-01, treatment of normal human melanocytes (Figures S3C and S3D), UACC62 human melanoma cells, and UACC257 human melanoma cells (Figures S1B, S1C, S1E, and S1F) with YKL 06-061 or YKL 06-062 for 3 hr yielded a dose-dependent increase in MITF mRNA expression. Levels of *TRPM1* mRNA increased after MITF induction upon treatment with YKL 06-061 or YKL 06-062 in normal human melanocytes and UACC257 human melanoma cells (Figures S1G, S1H, S3E, and S3F).

Topical SIK Inhibitors Induce Human Skin Eumelanization

Treatment of human skin explants with passive topical application of the second-generation SIK inhibitors, YKL 06-061 and YKL 06-062, induced significant pigmentation after 8 days of treatment (1×/day), but no significant gross pigmentation was observed in skin treated with HG 9-91-01 (Figure 4A). Fontana-Masson staining revealed increased melanin content in skin treated with YKL 06-061 or YKL 06-062 and marginally increased melanin in skin treated with HG 9-91-01, as compared with control (Figure 4B). This effect was reproducible with independent preparations of synthesized drugs applied passively (via pipette) to the top of different human skin explants (Figure 4C and 4D). Mechanical application of the first-generation SIK inhibitor HG 9-91-01, by rubbing via an applicator, induced significant gross pigmentation (Figure 4E), and increased melanin content was observed upon Fontana-Masson staining of skin sections (Figure 4F), suggesting that HG 9-91-01's limited human skin penetration can be, at least partially, overcome through mechanical application. YKL 06-061 and YKL 06-062 did not require

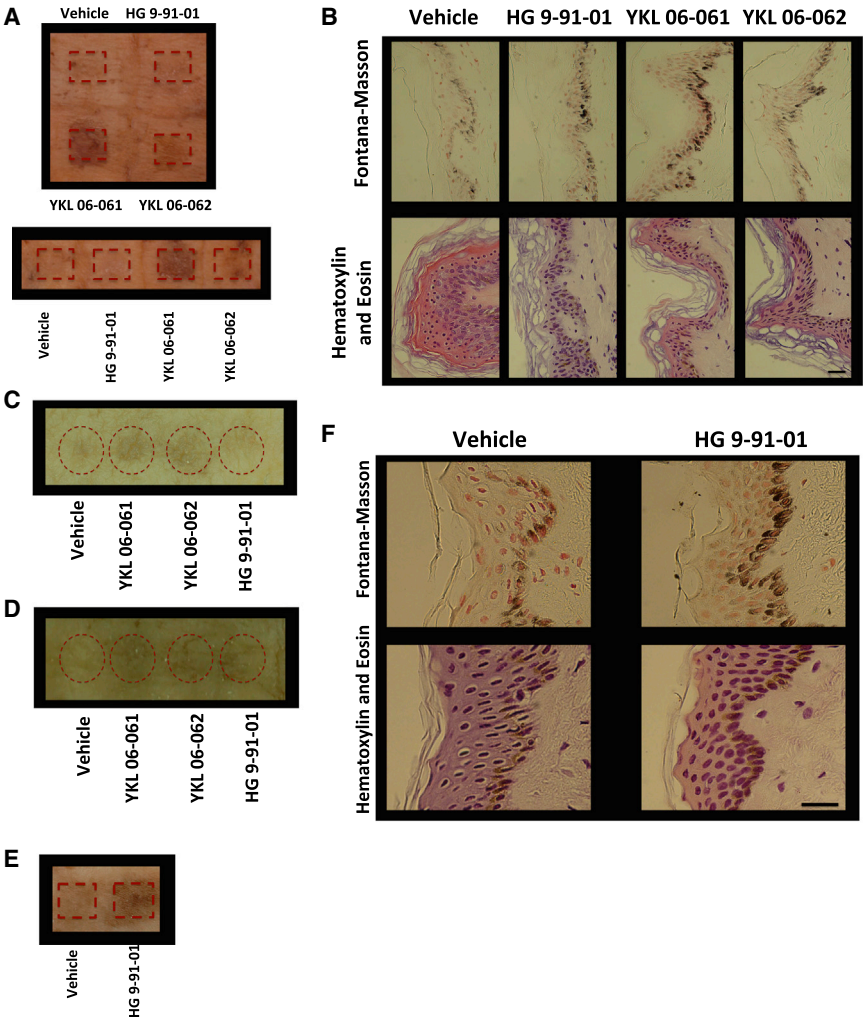

Figure 4. Treatment of Human Skin Explants with 37.5 mM of SIK Inhibitor Induces Pigmentation

(A) Human breast skin explants treated with passive application of vehicle control (70% ethanol, 30% propylene glycol) or 37.5 mM SIK inhibitor YKL 06-061, YKL 06-062, or HG 9-91-01 for 8 days (10 μL; 1×/day). Image was taken 2 days after the end of treatment (image is representative of two of n = 3 experiments).

(B) Fontana-Masson (top panel) and H&E (bottom panel) staining (magnification, 400×) of breast skin described in (A). Scale bar represents 25 μm.

(C) Human breast skin explants treated with passive application of vehicle control or 37.5 mM SIK inhibitor YKL 06-061, YKL 06-062, or HG 9-91-01 for 5 days (10 μL; 2×/day). Image was taken 1 day after the end of treatment (image is representative of n = 1 experiment).

(D) Human breast skin explants treated with passive application of vehicle control or 37.5 mM SIK inhibitor YKL 06-061, YKL 06-062, or HG 9-91-01 for 6 days (10 μL; 2×/day). Image was taken 1 day after the end of treatment (image is representative of n = 1 experiment).

(E) Human breast skin explants treated with mechanical application of vehicle control or 50 mM (50 μL for 1 day; 1×/day) or 25 mM (50 μL for 3 days; 3×/day) HG 9-91-01. Image was taken 4 days after the start of treatment (image is representative of n = 1 experiment).

(F) Fontana-Masson (top panels) and H&E (bottom panels) staining (magnification, 400×) of human skin explants described in (E). Scale bar represents 25 μm.

mechanical application (rubbing) to induce significant human epidermal darkening.

DISCUSSION

These results illustrate the development and successful application of small-molecule SIK inhibitors for topical induction of skin pigmentation independently of UV irradiation in human skin. SIK inhibitors were shown to induce enhanced expression of the MITF transcription factor, which is known to regulate expression of numerous pigment enzymes that promote biosynthesis of eumelanin. A new generation of SIK inhibitors was developed, based on strategies for enhancing the likelihood of skin penetration through optimizing molecular size and lipophilicity. Two such SIK-targeted inhibitors, YKL 06-061 and YKL 06-062, were shown to induce similar responses both in vitro and when applied to human skin explants. In addition to upregulating mRNA levels of *MITF* and *TRPM1*, topical SIK inhibitors were seen to trigger the transfer of melanosomes into epidermal keratinocytes in a manner that recapitulates the perinuclear capping (subcellular localization) seen in normal human epidermal pigmentation. Thus, SIK-inhibitor treatments appear to induce not only synthesis of melanin but also melanosomal maturation, export, and localization features, even after import into keratinocytes. These features closely resemble the previously observed behavior of forskolin treatment in red-haired mice (D'Orazio et al., 2006).

Topical application of small-molecule, UV-independent pigment inducers has not yet been examined in humans and would require careful considerations of safety. For example, the induction of dark pigmentation is associated with the lowest risk of most skin cancers in humans (Armstrong and Kricker, 2001; Pennello et al., 2000), and this pigment synthesis is believed to be dependent upon MITF (Bertolotto et al., 1998). However, fixed genomic mutation or amplification of the *MITF* gene can be oncogenic in certain contexts (Bertolotto et al., 2011; Garraway et al., 2005; Yokoyama et al., 2011). Reversible upregulation of MITF, as reported here, is also likely to occur in routine instances of UV tanning, and constitutive elevation of MITF is likely in the skin of individuals with darker pigmentation levels; neither would be anticipated to trigger genomic mutation of the *MITF* gene. Analogously, transient administration of recombinant hematopoietic growth factors has not been associated with formation of oncogenic transformation or leukemia (Dombret et al., 1995; Ohno et al., 1990). In mice, topical

forskolin's pigmentary rescue in "redheads" resulted in significant protection from UV carcinogenesis, without apparent associated toxicities over many months of treatment (D'Orazio et al., 2006). A recent study has utilized injections of the synthetic alpha-MSH analog, afamelanotide, for treatment of photosensitivity associated with erythropoietic protoporphyria. Pigmented lesions/melanoma were carefully evaluated and reported not to occur at elevated risk (Langendonk et al., 2015).

Our in vivo studies demonstrate that topical SIK inhibitor can be applied with localized SIK inhibition and no detected systemic effects in mice (such as failure to thrive); and although it has been previously shown that SIK1 inhibition leads to cell-cycle arrest in epithelial cells, this was dependent on the presence of transforming growth factor β (TGF-β) (Lönn et al., 2012), and we observed normal skin turnover with no morphological changes of the skin (measured grossly or histologically, other than pigment/color). During normal UV-induced tanning, MC1R activation leads to enhanced PKA activity (Newton et al., 2005), and PKA-dependent phosphorylation of SIK1 (Takemori et al., 2002), SIK2 (Horike et al., 2003), and SIK3 (Katoh et al., 2006) decreases their kinase activity. Since our compounds' activity is analogous to the on/off switch of UV-induced tanning, we believe that it will be a safe, viable method of topical pigment production, though it may be important to assure localized delivery to skin.

The half-life of melanin in skin is thought to be several weeks and diminishes primarily after superficial keratinocyte sloughing. Most epidermal melanin resides within keratinocytes after transfer of melanosomes from melanocytes. Therefore, it is possible that small-molecule approaches like that described here might be achievable, or maintained, through intermittent pulse-dosing strategies, thereby further limiting systemic drug exposure. In conclusion, these studies describe a small-molecule, topical approach to the rescue of eumelanin synthesis in a UV-independent manner. Future studies will be needed to examine the optimal applications of such agents in a variety of clinical settings.

EXPERIMENTAL PROCEDURES

See the Supplemental Information for detailed methods.

Materials

SIK inhibitors were dissolved in 30% propylene glycol plus 70% ethanol. HG 9-91-01 was purchased from Medchem Express, and all other SIK inhibitors were synthesized by the authors.

Kinome Profiling

Kinome profiling was performed using KinomeScan ScanMAX at a compound concentration of 1 μM. Data are reported in the Supplemental Information. Protocols are available from DiscoverX.

Kinase Activity In Vitro Assay

The biochemical activities against SIK2 were measured with a Caliper-based mobility shift assay (PerkinElmer).

Real-Time qPCR

The relative expression of each gene was calculated with 7500 Fast Real-Time PCR System software, which utilizes *Ct* normalized to mRNA levels of *RPL11* to calculate relative expression. Results are reported relative to control cells.

Mice

C57BL/6J $Mc1r^{e/e}$ mice were crossed with K14-SCF transgenic mice, and C57BL/6J $Tyr^{c2j/c2j}$ were crossed with K14-SCF transgenic mice (D'Orazio et al., 2006; Kunisada et al., 1998). Mixed-gender adult mice were used. All animal experiments were performed in accordance with institutional policies and Institutional Animal Care and Use Committee-approved protocols.

Human Tissue Samples

Skin samples considered surgical waste were obtained de-identified from healthy donors undergoing reconstructive surgery, according to institutional regulation.

Colorimeter Measurements

Differences in darkening of the skin were measured by reflective colorimetry (Commission Internationale de l'Eclairage [CIE] L* white-black color axis) utilizing a CR-400 Colorimeter (Minolta) calibrated to a white standard background calibration plate, with calibration date set to Y 93.1, x 0.3133, y 0.3194, before each set of measurements.

Statistical Analysis

Data are presented as the mean ± SEM.

Statistical significance of differences between experimental groups for in vitro experiments of cell lines treated with varying doses of SIKi or vehicle control were assessed by one-way ANOVA with Dunnett's multiple comparisons post-test. In vitro time course experiments were assessed by repeated-measures one-way ANOVA with Dunnett's multiple comparisons post-test.

Statistical significance for colorimeter readings in Figure 2B was determined by multiple t test analysis between day 0 and day 7 for each treatment group, with the two-stage linear step-up procedure of Benjamini, Krieger, and Yekutieli to correct for false discovery rate (FDR)—desired FDR (Q) = 1%—with no assumption of consistent SD. Statistical significance for colorimeter readings in Figure S3B were assessed by one-way ANOVA with Dunnett's multiple comparisons post-test.

For the G361 melanoma cells transduced with LKB1, a one-way ANOVA was used, with Dunnett's multiple comparisons test to assess the statistical significance of LKB1 expression and a two-tailed paired t test to assess the statistical significance of MITF induction with SIK-inhibitor treatment.

Statistical significance of differences between experimental groups for in vivo time course experiments was assessed by two-way ANOVAs with Sidak's multiple comparisons test.

Multiplicity-adjusted p values were reported for each comparison, and differences of means were considered significant if $p < 0.05$.

SUPPLEMENTAL INFORMATION

Supplemental Information includes Supplemental Experimental Procedures, three figures, and one data file and can be found with this article online at http://dx.doi.org/10.1016/j.celrep.2017.05.042.

AUTHOR CONTRIBUTIONS

N.M., Y.L., R.M., N.S.G., and D.E.F. contributed to conception and design of the study; N.M., Y.L., H.G.C., A.S.D., J.W., Y.S., Q.Y.W., J.A., L.V.K., A.L.H., and E.M.R. contributed to acquisition and analysis of data. N.M., D.E.F., and J.W. wrote the article.

ACKNOWLEDGMENTS

The authors thank Nicholas Lowe, Xunwei Wu, Jie Wen, Yang Feng, and Vivien Igras for technical advice and assistance. This work was supported by grants from NIH (5P01 CA163222 and 5R01 AR043369-19), the Melanoma Research Alliance, the Dr. Miriam and Sheldon G. Adelson Medical Research Foundation, and the Canadian Institutes of Health Research (DFS-140391).

N.M., R.M., N.S.G., and D.E.F. declare that parts of the work are subject of a U.S. provisional patent application titled "Pyrimidopyrimidinones as SIK Inhibitors."

Received: March 16, 2017
Revised: May 2, 2017
Accepted: May 12, 2017
Published: June 13, 2017

REFERENCES

Armstrong, B.K., and Kricker, A. (2001). The epidemiology of UV induced skin cancer. J. Photochem. Photobiol. B *63*, 8–18.

Bertolotto, C., Abbe, P., Hemesath, T.J., Bille, K., Fisher, D.E., Ortonne, J.P., and Ballotti, R. (1998). Microphthalmia gene product as a signal transducer in cAMP-induced differentiation of melanocytes. J. Cell Biol. *142*, 827–835.

Bertolotto, C., Lesueur, F., Giuliano, S., Strub, T., de Lichy, M., Bille, K., Dessen, P., d'Hayer, B., Mohamdi, H., Remenieras, A., et al.; French Familial Melanoma Study Group (2011). A SUMOylation-defective MITF germline mutation predisposes to melanoma and renal carcinoma. Nature *480*, 94–98.

Bos, J.D., and Meinardi, M.M. (2000). The 500 dalton rule for the skin penetration of chemical compounds and drugs. Exp. Dermatol. *9*, 165–169.

Choy, Y.B., and Prausnitz, M.R. (2011). The rule of five for non-oral routes of drug delivery: ophthalmic, inhalation and transdermal. Pharm. Res. *28*, 943–948.

Clark, K., MacKenzie, K.F., Petkevicius, K., Kristariyanto, Y., Zhang, J., Choi, H.G., Peggie, M., Plater, L., Pedrioli, P.G., McIver, E., et al. (2012). Phosphorylation of CRTC3 by the salt-inducible kinases controls the interconversion of classically activated and regulatory macrophages. Proc. Natl. Acad. Sci. USA *109*, 16986–16991.

Cui, R., Widlund, H.R., Feige, E., Lin, J.Y., Wilensky, D.L., Igras, V.E., D'Orazio, J., Fung, C.Y., Schanbacher, C.F., Granter, S.R., and Fisher, D.E. (2007). Central role of p53 in the suntan response and pathologic hyperpigmentation. Cell *128*, 853–864.

D'Orazio, J.A., Nobuhisa, T., Cui, R., Arya, M., Spry, M., Wakamatsu, K., Igras, V., Kunisada, T., Granter, S.R., Nishimura, E.K., et al. (2006). Topical drug rescue strategy and skin protection based on the role of Mc1r in UV-induced tanning. Nature *443*, 340–344.

Dombret, H., Chastang, C., Fenaux, P., Reiffers, J., Bordessoule, D., Bouabdallah, R., Mandelli, F., Ferrant, A., Auzanneau, G., Tilly, H., et al.; AML Cooperative Study Group (1995). A controlled study of recombinant human granulocyte colony-stimulating factor in elderly patients after treatment for acute myelogenous leukemia. N. Engl. J. Med. *332*, 1678–1683.

Gandini, S., Sera, F., Cattaruzza, M.S., Pasquini, P., Picconi, O., Boyle, P., and Melchi, C.F. (2005). Meta-analysis of risk factors for cutaneous melanoma: II. Sun exposure. Eur. J. Cancer *41*, 45–60.

Garraway, L.A., Widlund, H.R., Rubin, M.A., Getz, G., Berger, A.J., Ramaswamy, S., Beroukhim, R., Milner, D.A., Granter, S.R., Du, J., et al. (2005). Integrative genomic analyses identify MITF as a lineage survival oncogene amplified in malignant melanoma. Nature *436*, 117–122.

Horike, N., Takemori, H., Katoh, Y., Doi, J., Min, L., Asano, T., Sun, X.J., Yamamoto, H., Kasayama, S., Muraoka, M., et al. (2003). Adipose-specific expression, phosphorylation of Ser794 in insulin receptor substrate-1, and activation in diabetic animals of salt-inducible kinase-2. J. Biol. Chem. *278*, 18440–18447.

Horike, N., Kumagai, A., Shimono, Y., Onishi, T., Itoh, Y., Sasaki, T., Kitagawa, K., Hatano, O., Takagi, H., Susumu, T., et al. (2010). Downregulation of SIK2 expression promotes the melanogenic program in mice. Pigment Cell Melanoma Res. *23*, 809–819.

Katoh, Y., Takemori, H., Lin, X.Z., Tamura, M., Muraoka, M., Satoh, T., Tsuchiya, Y., Min, L., Doi, J., Miyauchi, A., et al. (2006). Silencing the constitutive active transcription factor CREB by the LKB1-SIK signaling cascade. FEBS J. *273*, 2730–2748.

Kennedy, C., Bajdik, C.D., Willemze, R., De Gruijl, F.R., and Bouwes Bavinck, J.N.; Leiden Skin Cancer Study (2003). The influence of painful sunburns and lifetime sun exposure on the risk of actinic keratoses, seborrheic warts, melanocytic nevi, atypical nevi, and skin cancer. J. Invest. Dermatol. *120*, 1087–1093.

Khaled, M., Levy, C., and Fisher, D.E. (2010). Control of melanocyte differentiation by a MITF-PDE4D3 homeostatic circuit. Genes Dev. *24*, 2276–2281.

Kobayashi, N., Nakagawa, A., Muramatsu, T., Yamashina, Y., Shirai, T., Hashimoto, M.W., Ishigaki, Y., Ohnishi, T., and Mori, T. (1998). Supranuclear melanin caps reduce ultraviolet induced DNA photoproducts in human epidermis. J. Invest. Dermatol. *110*, 806–810.

Kunisada, T., Lu, S.Z., Yoshida, H., Nishikawa, S., Nishikawa, S., Mizoguchi, M., Hayashi, S., Tyrrell, L., Williams, D.A., Wang, X., and Longley, B.J. (1998). Murine cutaneous mastocytosis and epidermal melanocytosis induced by keratinocyte expression of transgenic stem cell factor. J. Exp. Med. *187*, 1565–1573.

Langendonk, J.G., Balwani, M., Anderson, K.E., Bonkovsky, H.L., Anstey, A.V., Bissell, D.M., Bloomer, J., Edwards, C., Neumann, N.J., Parker, C., et al. (2015). Afamelanotide for erythropoietic protoporphyria. N. Engl. J. Med. *373*, 48–59.

Lipinski, C.A., Lombardo, F., Dominy, B.W., and Feeney, P.J. (2001). Experimental and computational approaches to estimate solubility and permeability in drug discovery and development settings. Adv. Drug Deliv. Rev. *46*, 3–26.

Lönn, P., Vanlandewijck, M., Raja, E., Kowanetz, M., Watanabe, Y., Kowanetz, K., Vasilaki, E., Heldin, C.H., and Moustakas, A. (2012). Transcriptional induction of salt-inducible kinase 1 by transforming growth factor β leads to negative regulation of type I receptor signaling in cooperation with the Smurf2 ubiquitin ligase. J. Biol. Chem. *287*, 12867–12878.

Miller, A.J., Du, J., Rowan, S., Hershey, C.L., Widlund, H.R., and Fisher, D.E. (2004). Transcriptional regulation of the melanoma prognostic marker melastatin (TRPM1) by MITF in melanocytes and melanoma. Cancer Res. *64*, 509–516.

Newton, R.A., Smit, S.E., Barnes, C.C., Pedley, J., Parsons, P.G., and Sturm, R.A. (2005). Activation of the cAMP pathway by variant human MC1R alleles expressed in HEK and in melanoma cells. Peptides *26*, 1818–1824.

Ohno, R., Tomonaga, M., Kobayashi, T., Kanamaru, A., Shirakawa, S., Masaoka, T., Omine, M., Oh, H., Nomura, T., Sakai, Y., et al. (1990). Effect of granulocyte colony-stimulating factor after intensive induction therapy in relapsed or refractory acute leukemia. N. Engl. J. Med. *323*, 871–877.

Park, S.B., Suh, D.H., and Youn, J.I. (1999). A long-term time course of colorimetric evaluation of ultraviolet light-induced skin reactions. Clin. Exp. Dermatol. *24*, 315–320.

Pennello, G., Devesa, S., and Gail, M. (2000). Association of surface ultraviolet B radiation levels with melanoma and nonmelanoma skin cancer in United States blacks. Cancer Epidemiol. Biomarkers Prev. *9*, 291–297.

Price, E.R., Horstmann, M.A., Wells, A.G., Weilbaecher, K.N., Takemoto, C.M., Landis, M.W., and Fisher, D.E. (1998). Alpha-melanocyte-stimulating hormone signaling regulates expression of microphthalmia, a gene deficient in Waardenburg syndrome. J. Biol. Chem. *273*, 33042–33047.

Rogers, H.W., Weinstock, M.A., Feldman, S.R., and Coldiron, B.M. (2015). Incidence estimate of nonmelanoma skin cancer (keratinocyte carcinomas) in the U.S. population, 2012. JAMA Dermatol. *151*, 1081–1086.

Ryerson, A.B., Eheman, C.R., Altekruse, S.F., Ward, J.W., Jemal, A., Sherman, R.L., Henley, S.J., Holtzman, D., Lake, A., Noone, A.M., et al. (2016). Annual report to the nation on the status of cancer, 1975-2012, featuring the increasing incidence of liver cancer. Cancer *122*, 1312–1337.

Takemori, H., Katoh, Y., Horike, N., Doi, J., and Okamoto, M. (2002). ACTH-induced nucleocytoplasmic translocation of salt-inducible kinase. Implication in the protein kinase A-activated gene transcription in mouse adrenocortical tumor cells. J. Biol. Chem. *277*, 42334–42343.

Tsatmalia, M., Wakamatsu, K., Graham, A.J., and Thody, A.J. (1999). Skin POMC peptides. Their binding affinities and activation of the human MC1 receptor. Ann. N Y Acad. Sci. *885*, 466–469.

Valverde, P., Healy, E., Jackson, I., Rees, J.L., and Thody, A.J. (1995). Variants of the melanocyte-stimulating hormone receptor gene are associated with red hair and fair skin in humans. Nat. Genet. *11*, 328–330.

Wakamatsu, K., and Ito, S. (2002). Advanced chemical methods in melanin determination. Pigment Cell Res. *15*, 174–183.

Watson, M., Geller, A.C., Tucker, M.A., Guy, G.P., Jr., and Weinstock, M.A. (2016). Melanoma burden and recent trends among non-Hispanic whites aged 15-49 years, United States. Prev. Med. *91*, 294–298.

Wu, S., Han, J., Vleugels, R.A., Puett, R., Laden, F., Hunter, D.J., and Qureshi, A.A. (2014). Cumulative ultraviolet radiation flux in adulthood and risk of incident skin cancers in women. Br. J. Cancer *110*, 1855–1861.

Yokoyama, S., Woods, S.L., Boyle, G.M., Aoude, L.G., MacGregor, S., Zismann, V., Gartside, M., Cust, A.E., Haq, R., Harland, M., et al. (2011). A novel recurrent mutation in MITF predisposes to familial and sporadic melanoma. Nature *480*, 99–103.

Cell Reports, Volume *19*

Supplemental Information

A UV-Independent Topical Small-Molecule Approach for Melanin Production in Human Skin

Nisma Mujahid, Yanke Liang, Ryo Murakami, Hwan Geun Choi, Allison S. Dobry, Jinhua Wang, Yusuke Suita, Qing Yu Weng, Jennifer Allouche, Lajos V. Kemeny, Andrea L. Hermann, Elisabeth M. Roider, Nathanael S. Gray, and David E. Fisher

Supplemental Figure Legends

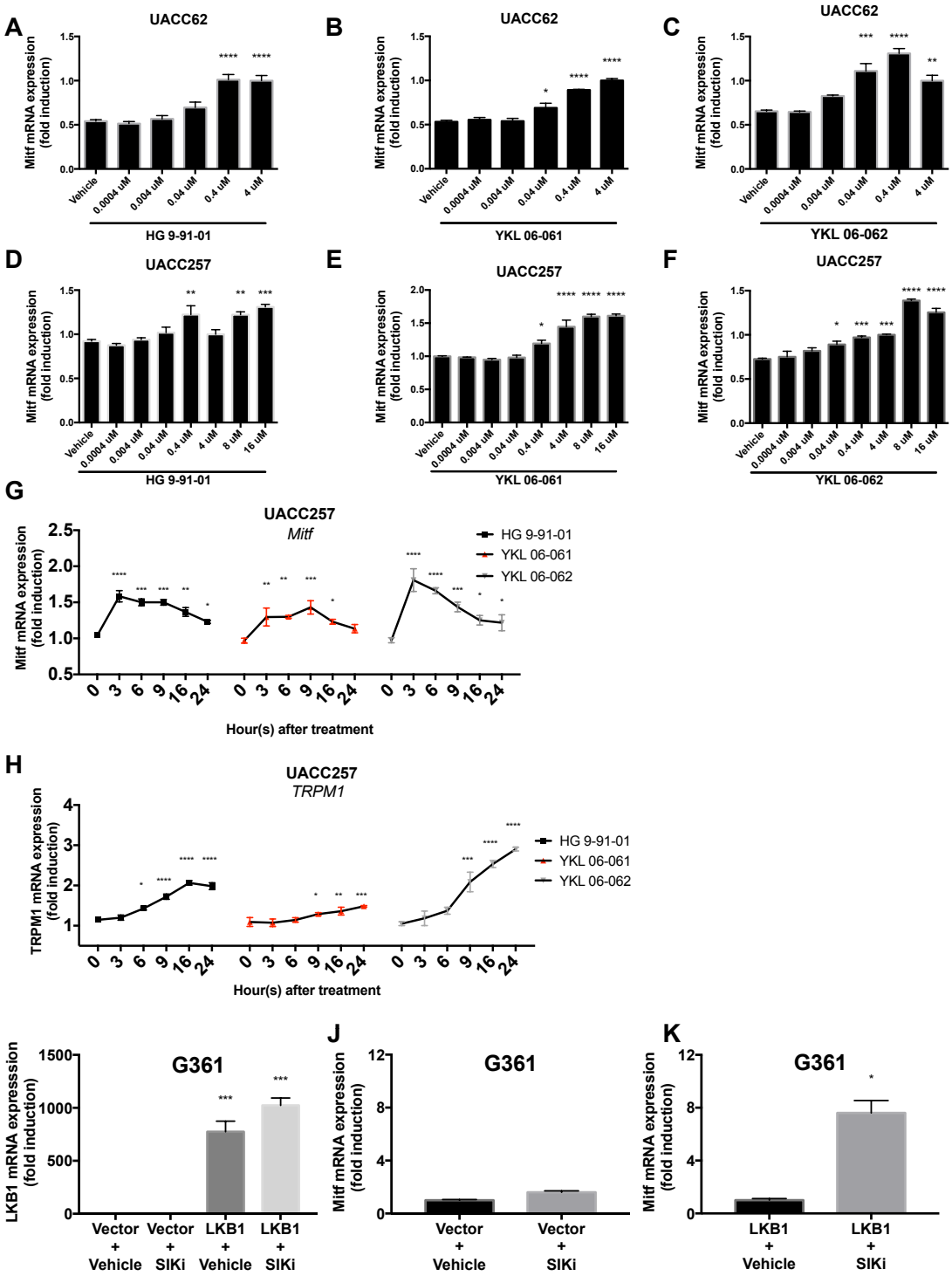

Figure S1: Inhibition of SIK by HG 9-91-01, YKL 06-061, and YKL 06-062 in UACC62 and UACC257 melanoma cells induces *MITF* expression. Related to Figure 1 and Figure 3. mRNA expression of *MITF* relative to *RPL11* mRNA and vehicle control quantified by qRT-PCR in human melanocytes, UACC62 melanoma cells **(A)**, **(B)**, **(C)** and UACC257 melanoma cells **(D)**, **(E)**, **(F)** treated with HG 9-91-01 **(A)**, **(D)**, YKL 06-061 **(B)**, **(E)**, or YKL 06-062 **(C)**, **(F)** (n=3, mean ± SEM). mRNA expression of *MITF* **(G)** and *MITF*-dependent gene *TRPM1* **(H)**, relative to *RPL11* and vehicle control (70% ethanol; 30% propylene glycol) at each time point, in normal human melanocytes treated with 4 μM of SIK inhibitor, quantified by qRT-PCR (n=3, mean ± SEM). **(I)** *LKB1* mRNA expression in G361 melanoma cells transduced with control vector or wild-type LKB1 overexpression vector (n=3, mean ± SEM). **(J)** *MITF* mRNA expression in control vector transduced G361 melanoma cells as described in **I** treated with 1 uM salt-inducible kinase inhibitor (SIKi) HG 9-91-01 or vehicle (dimethyl sulfoxide) (n=3, mean ± SEM). **(K)** *MITF* mRNA expression in LKB1 transduced G361 melanoma cells as described in **I** treated with 1 uM salt-inducible kinase inhibitor (SIKi) HG 9-91-01 or vehicle (dimethyl sulfoxide) (n=3, mean ± SEM). For graphs in **A**-**F**, statistical significance is reported as follows: *P < 0.05, **P < 0.01, ***P < 0.001, ****P < 0.0001, one-way ANOVA with Dunnett's multiple comparisons test comparing treatment dose to vehicle control. For graphs in **G** and **H**, statistical significance is reported as follows: *P < 0.05, **P < 0.01, ***P < 0.001, ****P < 0.0001, repeated measures one-way ANOVA with Dunnett's multiple comparisons test comparing each time point to time point zero. For graph in **I**, statistical significance is reported as follows: ***P < 0.001, one-way ANOVA with Dunnett's multiple comparisons test comparing all experimental groups to vector + vehicle experimental group. For graphs in **J** and **K**, statistical significance is reported as

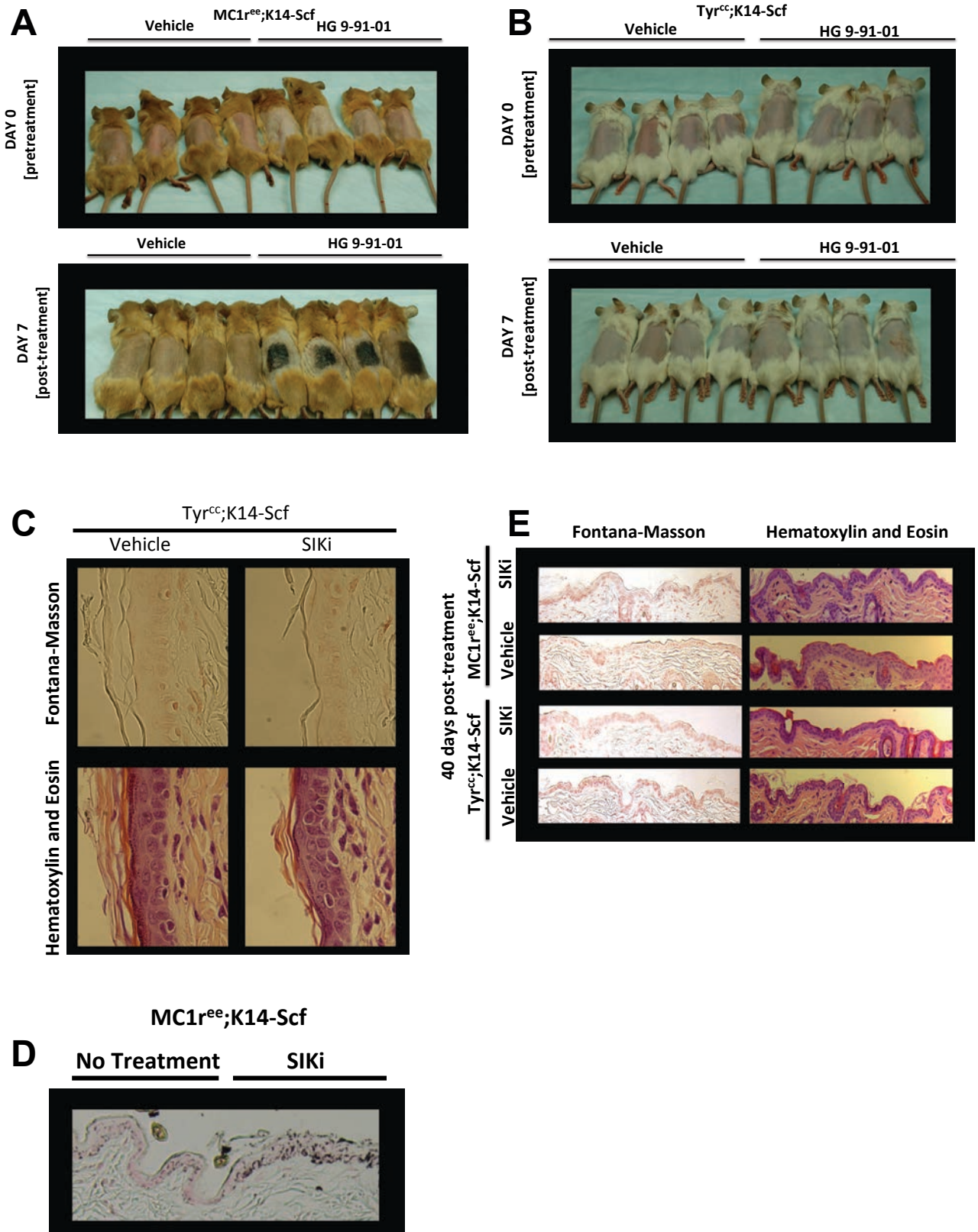

Figure S2: **Expansion of Figure 2**. *Mc1r*$^{e/e}$;K14-SCF mice **(A)** and *Tyr*$^{c/c}$;K14-SCF mice **(B)** before treatment (Day 0) and after 7 days of treatment (Day 7) with 30 µL of vehicle control (70% ethanol; 30% propylene glycol) or 37.5 mM HG 9-91-01 (image of all replicates of mice represented in **Figure 2A**). **(C)** Fontana-Masson (eumelanin) [top panel] and hematoxylin and eosin stains [bottom panel] of *Tyr*$^{c/c}$;K14-SCF mice as described in **Figure 2A** (x630 magnification) (image is representative of n=4 experiments). Fontana-Masson (eumelanin) stained skin sections of *Mc1r*$^{e/e}$;K14-SCF mice treated with 37.5 mM HG 9-91-01 for 7 days as described in **Figure 2A**. **(D)** Image is at the margin of treated and untreated area (x100 magnification). **(E)** Fontana-Masson (eumelanin) [left panels] and hematoxylin and eosin stains [right panels] of *Mc1R*$^{e/e}$;K14-SCF mice and *Tyr*$^{c/c}$;K14-SCF mice with vehicle or 37.5 mM HG 9-91-01 as described **Figure 2E** (x200 magnification)**.**

A

Molecule Name	Molecular weight (g/mol)	CLogP	H-bond donors	H-bond acceptors
HG-9-91-01	567.681	6.01	2	8
HG-11-137-01	429.518	3.34	1	6
HG-11-139-02	459.544	3.19	1	7
YKL-05-201-1	447.917	4.74	1	5
YKL-06-029	457.571	4.37	1	6
YKL-06-059	515.65	4.99	1	7
YKL-06-060	497.634	5.28	1	6
YKL-06-061	527.66	5.12	1	7
YKL-06-062	525.688	6.17	1	6

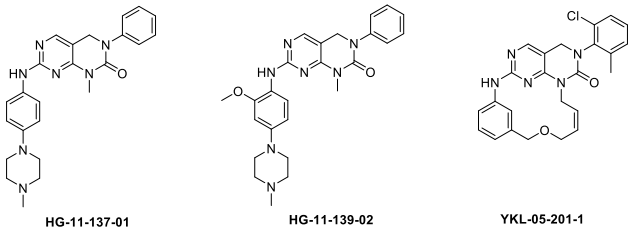

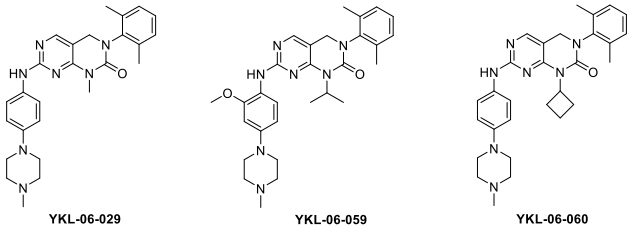

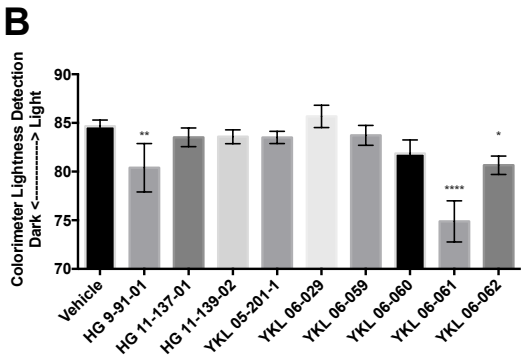

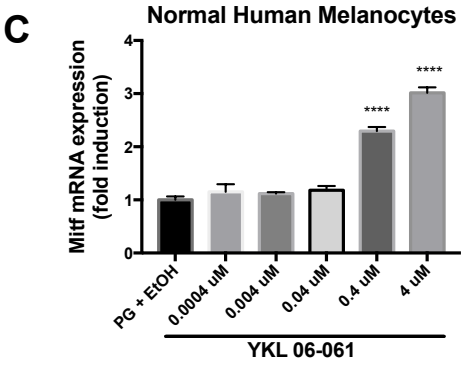

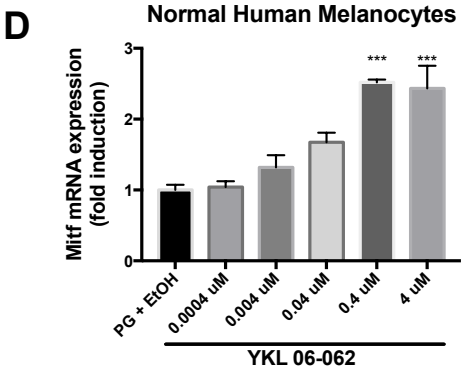

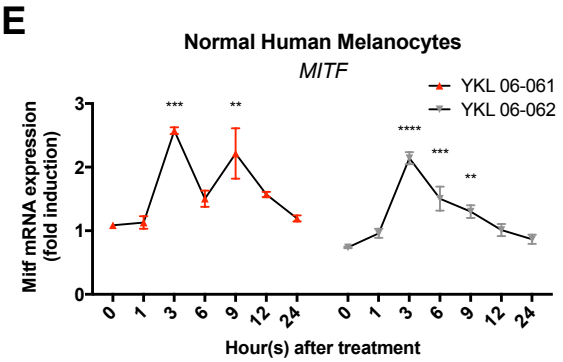

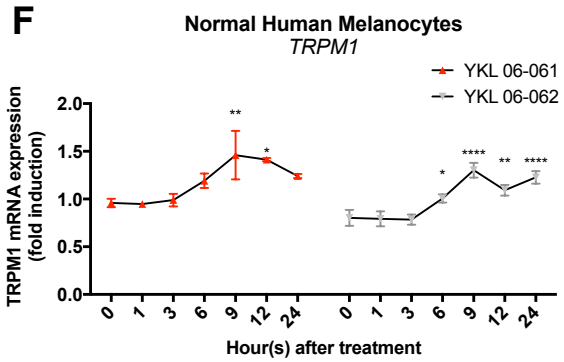

Figure S3: Second generation SIK inhibitors are as efficacious in inducing the pigmentation pathway as HG 9-91-01. Related to Figure 3. **(A)** Physiochemical properties of SIK inhibitors and structures of SIK inhibitors HG 11-137-01, HG 11-139-02, YKL 05-201-1, YKL 06-029, YKL 06-059, YKL 06-060 **(B)** Reflective colorimetry measurements (L* white-black color axis) of human breast skin explants treated with passive application of vehicle control (70% ethanol; 30% propylene glycol) or 37.5 mM of SIK inhibitors HG 9-91-01, HG 11-137-01, HG 11-139-02, YKL 05-201-1, YKL 06-029, YKL 06-059, YKL 06-060, YKL 06-061, or YKL 06-062 for 8 days (30 uL; 2x/day). Colorimeter analysis 1 day after end of treatment (n=3, mean ± SEM). mRNA expression of *MITF* relative to *RPL11* mRNA and vehicle control in normal human melanocytes, treated with YKL 06-061 **(C),** YKL 06-062 **(D)**, or vehicle control (70% ethanol; 30% propylene glycol) **(C,D)**, quantified by qRT-PCR (n=3, mean ± SEM). mRNA expression of *MITF* **(E)** and *MITF*-dependent gene *TRPM1* **(F)** relative to *RPL11* and vehicle control at each time point, in normal human melanocytes over 24 hours after 4 μM YKL 06-061, YKL 06-062, or vehicle control treatment, quantified by qRT-PCR (n=3, mean ± SEM). For graph in **B**, statistical significance is reported as follows: *P < 0.05, **P < 0.01, ***P < 0.001, one-way ANOVA with Dunnett's multiple comparisons test comparing each treatment group to vehicle control. For graphs in **C** and **D**, statistical significance is reported as follows: ***P < 0.001, ****P < 0.0001, one-way ANOVA with Dunnett's multiple comparisons test comparing treatment dose to vehicle control. For graphs in **E** and **F**, statistical significance is reported as follows: *P < 0.05, **P < 0.01, ***P < 0.001, ****P < 0.0001, repeated measures one-way ANOVA with Dunnett's multiple comparisons test comparing each time point to

Supplemental Experimental Procedures

Quantitative real time polymerase chain reaction (qRT-PCR). mRNA was extracted from cells using the RNeasy Mini Kit (Qiagen). KAPA SYBR ® FAST Universal One-Step qRT-PCR Kit (KAPA BIOSYSTEMS) was used to prepare mRNA samples for qRT-PCR and samples were analyzed using the 7500 Fast Real Time PCR System (Applied Biosystems). The relative expression of each gene was calculated by 7500 Fast System Software, which utilizes *Ct* normalized to mRNA levels of *RPL11* to calculate relative expression. Results are reported relative to control cells. Primer sequences used: human M-specific *MITF* forward 5'-CATTGTTATGCTGGAAATGCTAGAA-3', human M-specific *MITF* reverse 5'-GGCTTGCTGTATGTGGTACTTGG-3', *TRPM1* forward 5'-ATGCCTTGAAAGACCACTCCTCCA-3', *TRPM1* reverse 5'-TGTGGGAGTTGTTGAGCACAGAGA-3', *RPL11* forward 5'- GTTGGGGAGAGTGGAGACAG-3', *RPL11* reverse 5'-TGCCAAAGGATCTGACAGTG-3'.

Kinase activity *in vitro* assay. The biochemical activities against SIK2 were measured by Caliper-based mobility shift assay (PerkinElmer). For these experiments, full length His6-MBP-tagged hSIK2 (4 nM) was incubated with HG-9-91-01 derivatives in buffer containing 100 mM HEPES 7.5, 10 mM $MgCl_2$, 2.5 mM DTT, 0.004% Tween 20, 0.003% Brij-35, 30 μM ATP, and 1.5 μM ProfilerPro FL-Peptide 10 (5-FAMKKKVSRSGLYRSPSMPENLNRPR-COOH, PerkinElmer, Catalog No. 760354) at room temperature. Reactions were quenched by adding 20 mM EDTA (pH 8) after 1 hour, and percentage of substrate conversion was measured by LabChip EZ Reader II (PerkinElmer). IC50s for SIK2 inhibition were calculated using SmartFit nonlinear regression in Genedata Screener software suite (Genedata).
All other *in vitro* kinase assay were conducted using the SelectScreen Kinase Profiling Service at Thermo Fisher Scientific (Madison, WI). The protocols are available from the Thermo Fisher Scientific website.

Cell Culture. UACC257 human melanoma cells and UACC62 human melanoma cells were grown in RPM1 medium + 1% penicillin/streptomycin/glutamine + 5% fetal bovine serum. Normal human melanocytes were grown in TIVA medium (HAM's F-12, 1% penicillin/streptomycin/glutamine, 10% fetal bovine serum, 50ng/mL 12-O-tetradecanoyl phorbol-13-acetate, 1 x 10^{-4} M 3-isobutyl-1-methyl xanthine, 1 μM Na_3VO_4, 1 x 10^{-3} M N^6,2'-O-dibutyryladenosine 3:5-cyclic monophosphate), and were starved for 24 hours in HAM's F-12 + 1% penicillin/streptomycin/glutamine before all molecular experiments.

Lentiviral Transduction. Lentivirus was produced by cotransfection of 293T cells with LKB1-expressing lentivirus vector, packaging system VSV-G (Cell Biolabs Inc), and psPAX2 (Addgene). 1 x 10^6 G361 melanoma cells were plated in each well of a 6-well plate. Cells were infected with virus in the presence of 8 ug/mL of polybrene infection reagent (Sigma-Aldrich). Plates were spun at room temperature for 1.5 hours at 1,000 RPM. Media was changed to viral-free media 24 hours after infection. 48 hours after infection cells were treated in 1 uM of SIKi or vehicle control (DMSO) and mRNA samples were collected after 3 hours.

Photos. Photos were taken using a Nikon D50 DSLR camera with a Nikon Nikkor 40 mm f/2.8 DX G AF-S lens. Shutter speed ranged from 1/40 to 1/250 and aperture ranged from F3-F8. Ott-Lite Model L139AB lamps were used to create uniform lighting for photos.

Cell pelleting experiments. 1x10^5 UACC257 cells were plated per well in a 6-well plate. Cells were treated daily (1x/day) with 4 μM of SIK inhibitor HG 9-91-01 or vehicle control (30% propylene glycol + 70% ethanol). After 3 days, cells were detached with 0.25% trypsin, resuspended in RPMI media, and centrifuged. RPMI media was removed and pellets were washed 1x with PBS and allowed to dry before imaging.

Mouse pigmentation experiments. For *in vivo* darkening experiment, male and female mice ranging from 1.5-3 months old were used. For *in vivo* time course experiment, male and female mice ranging from 2.5-6 months were used. Animals were waxed and treated with vehicle control (30% propylene glycol + 70% ethanol) or 37.5 mM HG 9-9-01 until uniform gross darkening was visible, as stated in figure legends. Daily differences in darkening of the skin were measured by reflective colorimetry (when hair was re-growing, no measurement was taken until hair was long enough to be waxed). Skin was harvested, fixed, and processed for paraffin embedding. Sections were cut from paraffin blocks, and sections were stained utilizing hematoxylin and eosin (morphology) and Fontana-Masson (melanin). Melanin dissolution was conducted utilizing the NaOH lysis method as described previously by Wakamatsu and Ito. In the time course experiment, one vehicle-treated *Tyr*$^{c/c}$;K14-SCF mouse (Day 11) and two vehicle-treated *Mc1r*$^{e/e}$;K14-SCF mice (Day 23 and Day 34) died due to technical reasons.

Human pigmentation experiments. Full thickness human breast skin explants were cultured in petri dishes with a solid phase and liquid phase phenol red free DMEM medium with 20% penicillin/streptomycin/glutamine, 5% fungizone (Gibco), and 10% fetal bovine serum. Explants were treated daily with vehicle or SIK inhibitor as indicated in figure legends. Passive application refers to simply applying the treatment to skin without further rubbing or manipulation. Mechanical application refers to application of agents to skin with further rubbing of treatment with 10 clockwise turns of a gloved cotton swab applicator. Skin was harvested, fixed, and processed for paraffin embedding. Sections were cut from paraffin blocks, and sections were stained utilizing hematoxylin and eosin (morphology) and Fontana-Masson (melanin).

Synthetic procedure of small molecule SIK inhibitors:
Unless otherwise noted, reagents and solvents were used as received from commercial suppliers. Proton nuclear magnetic resonance spectra were obtained on Bruker AVANCE spectrometer at 400 MHz for proton. Spectra are given in ppm (δ) and coupling constants, J, are reported in Hertz. The solvent peak was used as the reference peak for proton spectra. LC-MS spectra were obtained on Agilent 1100 HPLC LC-MS ion trap electrospray ionization (ESI) mass spectrometer.

Synthesis of YKL-06-061

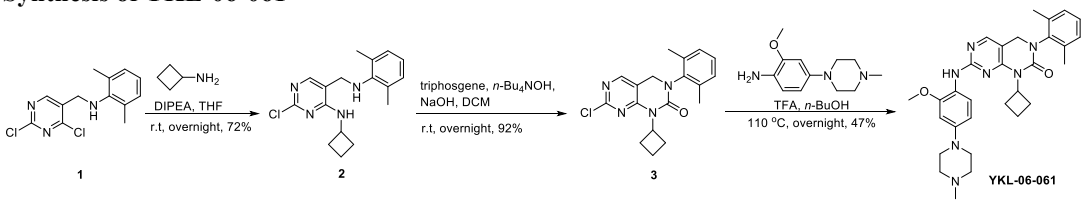

2-chloro-N-cyclobutyl-5-((2,6-dimethylphenylamino)methyl)pyrimidin-4-amine (2)
A mixture of N-((2,4-dichloropyrimidin-5-yl)methyl)-2,6-dimethylaniline **(1)** (1.10 g, 3.91 mmol), cyclobutanamine (1.67 g, 23.49 mmol) and DIPEA (6 mL) in THF (100 mL) was stirred at room temperature overnight. Then the mixture was concentrated, the residue was purified by flash column (eluting with ethyl acetate /PE = 0-15%) to give 2-chloro-N-cyclobutyl-5-((2,6-dimethylphenylamino)methyl)pyrimidin-4-amine **(2)** as white solid (0.90 g, yield 72%). LCMS (m/z): 317 $[M + H]^+$.
7-chloro-1-cyclobutyl-3-(2,6-dimethylphenyl)-3,4-dihydropyrimido[4,5-d]pyrimidin-2(1H)-one (3)
A mixture of 2-chloro-N-cyclobutyl-5-((2,6-dimethylphenylamino)methyl)pyrimidin-4-amine **(2)** (0.75 g, 2.37 mmol) and triphosgene (1.05 g, 3.56 mmol) in DCM (100 mL) was stirred at room temperature for 1 hour, the a solution of NaOH (1.90 g, 47.5 mmol) and *n*-Bu_4NOH (78 mg, 0.301 mmol) in H_2O (24 mL) was added, the resulting mixture was stirred at room temperature overnight. The organic layer was washed with H_2O (50 mL × 2), dried with Na_2SO_4, filtered and concentrated, the residue was purified by flash column (eluting with ethyl acetate /PE = 0-15%) to give 7-chloro-1-cyclobutyl-3-(2,6-dimethylphenyl)-3,4-dihydropyrimido[4,5-d] pyrimidin-2(1H)-one **(3)** as white solid (750 mg, yield 92%). LCMS (m/z): 343 $[M + H]^+$. ^{1}H-NMR ($CDCl_3$, 400 MHz): δ 8.11 (s, 1H), 7.11-7.18 (m, 3H), 4.83-4.92 (m, 1H), 4.47 (d, *J* = 0.8Hz, 2H), 2.52-2.59 (m, 4H), 2.22 (s, 6H), 1.74-1.92 (m, 2H).
1-cyclobutyl-3-(2,6-dimethylphenyl)-7-(2-methoxy-4-(4-methylpiperazin-1-yl)phenylamino)-3,4-dihydropyrimido[4,5-d]pyrimidin-2(1H)-one (YKL-06-061)
A mixture of 7-chloro-1-cyclobutyl-3-(2,6-dimethylphenyl)-3,4-dihydropyrimido[4,5-d]pyrimidin-2(1H)-one **(3)** (70 mg, 0.204 mmol), 2-methoxy-4-(4-methylpiperazin-1-yl)aniline (66 mg, 0.298 mmol) and TFA (0.5 mL) in *n*-BuOH (5 mL) was stirred at 110°C overnight, the mixture was concentrated, the residue was purified by prep-HPLC (0.05%NH_4HCO_3 in CH_3CN-H_2O) to give **YKL-06-061** as white solid (50 mg, yield 47%). LCMS (m/z): 528 $[M + H]^+$. ^{1}H-NMR ($CDCl_3$, 400 MHz): δ 8.22 (d, *J* = 8.4 Hz, 1H), 7.95 (s, 1H), 7.36 (s, 1H), 7.09 - 7.16 (m, 3H), 6.56 - 6.60 (m, 2H), 4.90 - 4.98 (m, 1H), 4.37 (s, 2H), 3.90 (s, 3H), 3.20 (t, *J* = 5.2 Hz, 4H), 2.58 - 2.68 (m, 6H), 2.46-2.54 (m, 2H), 2.38 (s, 3H), 2.23 (s, 6H), 1.74-1.89 (m, 2H).

Synthesis of YKL-06-062

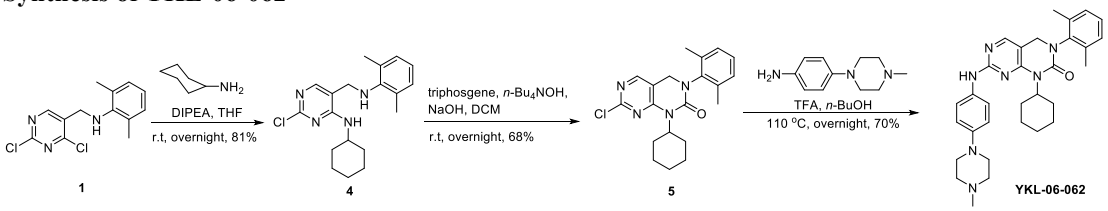

2-chloro-N-cyclohexyl-5-((2,6-dimethylphenylamino)methyl)pyrimidin-4-amine (4)
A mixture of A mixture of N-((2,4-dichloropyrimidin-5-yl)methyl)-2,6-dimethylaniline **(1)** (1.5g, 5.34 mmol), cyclohexanamine (3.17 g, 32.0 mmol) and DIPEA (6 mL) was stirred at room temperature overnight. Then the mixture was concentrated, the residue was purified by flash column (eluting with ethyl acetate /PE = 0-12%) to give 2-chloro-N-cyclohexyl-5-((2,6-dimethylphenylamino)methyl)pyrimidin-4-amine **(4)** as white solid (1.5 g, yield 81%). LCMS (m/z): 345 $[M + H]^+$.
7-chloro-1-cyclohexyl-3-(2,6-dimethylphenyl)-3,4-dihydropyrimido[4,5-d]pyrimidin-2(1H)-one (5)
A mixture of 2-chloro-N-cyclohexyl-5-((2,6-dimethylphenylamino)methyl)pyrimidin-4-amine **(4)** (1.50 g, 4.36 mmol) and triphosgene (1.94 g, 6.54 mmol) in DCM (100 mL) was stirred at room temperature for 30 minutes, then a solution of NaOH (3.49 g, 87.3 mmol) and n-Bu_4NOH (78 mg, 0.301 mmol) in H_2O (43 mL) was added, the resulting mixture was stirred at room temperature overnight. The organic layer was washed with H_2O (50 mL × 2), dried with Na_2SO_4, filtered and concentrated to give crude product, then purified by flash column (eluting with ethyl acetate /PE = 0-20%) to give 7-chloro-1-cyclohexyl-3-(2,6-dimethylphenyl)-3,4-dihydro-
pyrimido[4,5-d]pyrimidin-2(1H)-one **(5)** as white solid (1.1 g, yield 68%). LCMS (m/z): 371 $[M + H]^+$.
^{1}H-NMR ($CDCl_3$, 400 MHz): δ 8.08 (s, 1H), 7.11-7.18 (m, 3H), 4.63-4.71 (m, 1H), 4.49 (d, *J* = 0.8Hz, 2H), 2.45-2.56 (m, 2H), 2.22 (s, 6H), 1.65-1.86 (m, 5H), 1.34-1.43 (m, 2H), 1.17-1.28 (m, 1H).
1-cyclohexyl-3-(2,6-dimethylphenyl)-7-(4-(4-methylpiperazin-1-yl)phenylamino)-3,4-dihydropyrimido[4,5-d]pyrimidin-2(1H)-one (YKL-06-062)

A mixture of 7-chloro-1-cyclohexyl-3-(2,6-dimethylphenyl)-3,4-dihydropyrimido[4,5-d]pyrimidin-2(1H)-one **(5)** (94 mg, 0.254 mmol), 4-(4-methylpiperazin-1-yl)aniline (97 mg, 0.508 mmol) and TFA (0.5 mL) in *n*-BuOH (8 mL) was stirred at 110°C overnight. The mixture was concentrated, the residue was purified by prep-HPLC (0.05%NH_4HCO_3 in CH_3CN-H_2O) to give **YKL-06-062** as light yellow solid (94 mg, yield 70%). LCMS (m/z): 526 $[M + H]^+$. ^{1}H-NMR ($CDCl_3$, 400 MHz): δ 7.92 (s, 1H), 7.46 - 7.50 (m, 2H), 7.09 - 7.15 (m, 3H), 7.02 (s, 1H), 6.93 - 6.96 (m, 2H), 4.61 - 4.69 (m, 1H), 4.38 (s, 2H), 3.19 (t, *J* = 5.2 Hz, 4H), 2.61 (t, *J* = 5.2 Hz, 4H), 2.43-2.53 (m, 2H), 2.36 (s, 3H), 2.23 (s, 6H), 1.76 - 1.86 (m, 4H), 1.66 (d, *J* = 12.4 Hz, 1H), 1.32 - 1.43 (m, 2H), 1.14-1.23 (m, 1H).